The Effect of Phase Junction Structure on the Photocatalytic Performance in Overall Water Splitting: Ga 2 O 3 Photocatalyst as an Example

ARTICLE *in* THE JOURNAL OF PHYSICAL CHEMISTRY C · JULY 2015

Impact Factor: 4.77 · DOI: 10.1021/acs.jpcc.5b04092

THE JOURNAL OF PHYSICAL CHEMISTRY C

Article

pubs.acs.org/JPCC

Effect of Phase Junction Structure on the Photocatalytic Performance in Overall Water Splitting: Ga_2O_3 Photocatalyst as an Example

Shaoqing Jin,[†,‡] Xiang Wang,[†] Xiuli Wang,[†] Minggang Ju,[§] Shuai Shen,[†] Wanzhen Liang,[∥,⊥] Yi Zhao,[∥,⊥] Zhaochi Feng,[†] Helen Y. Playford,[#] Richard I. Walton,[#] and Can Li*[,†,⊥]

[†]State Key Laboratory of Catalysis, Dalian Institute of Chemical Physics, Chinese Academy of Sciences, Dalian 116023, China

[‡]University of the Chinese Academy of Sciences, Beijing 100049, China

[§]Department of Chemical Physics, University of Science and Technology of China, Hefei 230026, China

[∥]State Key Laboratory of Physical Chemistry of Solid Surfaces, Department of Chemistry, College of Chemistry and Chemical Engineering, Xiamen University, Xiamen 361005, China

[⊥]Collaborative Innovation Center of Chemistry for Energy Materials and [#]Department of Chemistry, University of Warwick, Coventry CV4 7AL, U.K.

Supporting Information

ABSTRACT: The fabrication of surface phase junctions has proven to be an efficient strategy for the enhancement of photocatalytic activity; however, some questions about these systems are not yet well understood. In this study, the photocatalytic overall water splitting reaction was achieved on photocatalysts with pure and mixed phase compositions of cubic γ-Ga_2O_3 and monoclinic β-Ga_2O_3. All the Ga_2O_3 photocatalysts can split water stoichiometrically into H_2 and O_2; however, the phase-mixed γ/β-Ga_2O_3 photocatalyst with a small amount of β phase shows the lowest activity. This is opposite from that of the reported α/β-Ga_2O_3 system in which the phase-mixed α/β-Ga_2O_3 photocatalyst with a small amount of β phase shows much higher photocatalytic activity than the individual phases. Much more disordered structure is found between the γ and β phases in the γ/β-Ga_2O_3 photocatalyst with low content of β phase due to the defective spinel structure of γ phase. Spectroscopic characterization and theoretical calculations indicate that the disordered structure serves as defect and charge recombination centers resulting in the decrease of photocatalytic activity. Based on the analysis of α/β-Ga_2O_3 and γ/β-Ga_2O_3 systems, it is proposed that a prerequisite for the formation of phase junction boosting photocatalytic reactions is that the interfacial structure between two phases should not be disordered or defective.

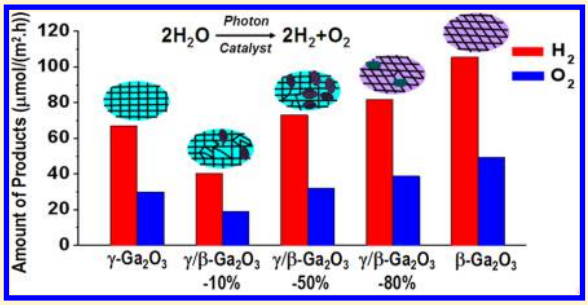

INTRODUCTION

Direct overall water splitting based on semiconductor photocatalysis is an appealing strategy for a sustainable hydrogen economy and has been attracting much attention.[1−4] However, photocatalytic overall water splitting encounters numerous scientific challenges since the performance of the photocatalyst is far from practical application and greatly affected by a number of factors.[5−10] In order to produce high-performance photocatalysts, the relationship between the structure of photocatalyst and its performance has been extensively investigated, such as the influence of crystal structure[11−15] and surface structure[5,16,17] on photocatalytic activity. In our previous work, with the surface phase characterized by UV Raman spectroscopy, we found that the photocatalytic activity of photocatalyst is surface phase-dependent and it could be enhanced by the presence of surface phase junction.[16,17] For example, the activity of TiO_2 is enhanced by surface anatase/rutile phase junction toward photocatalytic hydrogen evolution.[16] Furthermore, we found that the surface α/β phase junction of Ga_2O_3 can effectively promote photocatalytic overall water splitting.[17] The time-resolved spectroscopic study revealed that the enhancement of photocatalytic activity can be attributed to the promotion of charge separation by α/β Ga_2O_3 phase junction. Even so, there is still no very clear information about what are the necessities for the formation of phase junction being beneficial for photocatalytic reactions. This motivates us to carry out the study for a better and deeper understanding of phase junction.

As a representative polymorphic semiconductor, Ga_2O_3 with at least four polymorphs that have been structurally characterized (α-, β-, γ-, and ε-Ga_2O_3) has attracted much attention in the field of catalysis.[18−24] Among these polymorphs, β-Ga_2O_3 is the thermodynamically stable one, and all the other polymorphs can be ultimately transformed into β-Ga_2O_3 by calcination.[25,26] This indicates that Ga_2O_3 material is a suitable platform for the study of phase junction,

Received: April 29, 2015
Revised: July 20, 2015
Published: July 22, 2015

DOI: 10.1021/acs.jpcc.5b04092
J. Phys. Chem. C 2015, 119, 18221−18228

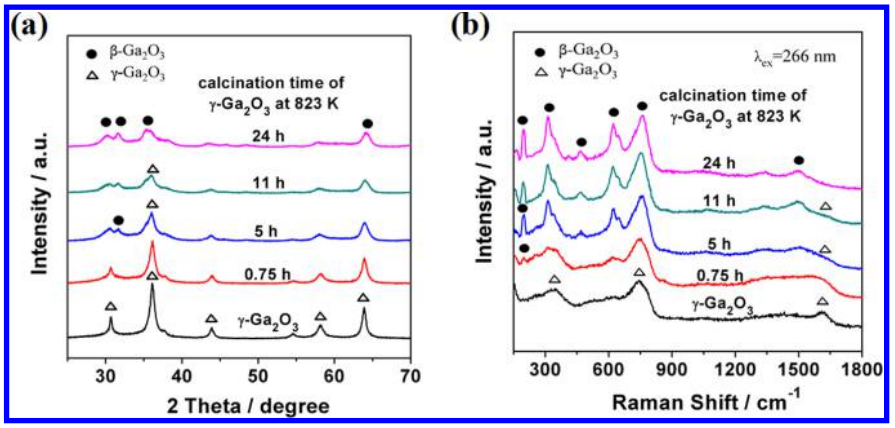

Figure 1. Powder XRD patterns (a) and 266 nm excited UV Raman spectra (b) of as-synthesized and calcined γ-Ga_2O_3 samples.

although only the α/β phase junction of Ga_2O_3 has so far been investigated.[17] In most cases, α-Ga_2O_3, β-Ga_2O_3, and γ-Ga_2O_3 were investigated individually to study the structure−performance relationship due to their easy preparation and definite structures.[18−20] Photocatalytic overall water splitting has been performed on α-Ga_2O_3 and β-Ga_2O_3;[17,27−30] however, no photocatalytic overall water splitting on γ-Ga_2O_3 has been reported yet, to our knowledge. The γ phase is defective in its structure, as a cubic spinel with partial filling of two octahedral and two tetrahedral sites whose site occupation may depend on synthesis method and particle size.[31] This is very different from α and β phases, with the former being an analogue of hexagonal α-Al_2O_3 with only octahedral gallium and the latter a unique monoclinic structure with fully occupied octahedral and tetrahedral sites for gallium.[26] Given the difference in structures, it would be helpful for a deep understanding of phase junction in semiconductor photocatalyst to study the phase-mixed γ/β-Ga_2O_3 system.

Therefore, in this study, we carried out the photocatalytic overall water splitting reaction on Ga_2O_3 photocatalysts with different composition of γ and β phases. We found that the phase structure of Ga_2O_3 photocatalyst greatly affects the reaction activity. Different from the interface between α-Ga_2O_3 and β-Ga_2O_3, disordered structure is formed between the two phases in the phase transformation of γ-Ga_2O_3 to β-Ga_2O_3, which shows a negative effect on photocatalytic overall water splitting. Spectroscopic characterization and theoretical calculations indicate that the disordered structure serves as defect and charge recombination centers resulting in the decrease of photocatalytic activity. Through the analysis of γ/β-Ga_2O_3 and reported α/β-Ga_2O_3 systems, we propose two requirements for the construction of phase junction boosting photocatalytic reactions.

EXPERIMENTAL SECTION

Preparation. γ-Ga_2O_3 was synthesized by solvothermal oxidation of gallium metal reported in the literature.[26] The other Ga_2O_3 samples were obtained by calcining γ-Ga_2O_3 at 823 K for different times (0.75, 5, 11, and 24 h) in air. $RhCl_3$ (Rh/Ga_2O_3 = 0.5 wt %) and the corresponding amount of $(NH_4)_2Cr_2O_7$ were used for the loading of $Rh_{0.5}Cr_{1.5}O_3$ cocatalyst on Ga_2O_3 photocatalysts by an impregnation method followed by calcination at 623 K for 1 h. Ni cocatalyst was loaded on γ-Ga_2O_3 and calcined γ-Ga_2O_3 (calcination time of 0.75, 24 h) samples by *in situ* photodeposition method with $Ni(NO_3)_2$ (Ni/Ga_2O_3 = 1 wt %) as the Ni source.

Characterization. Powder X-ray diffraction (XRD) patterns were recorded on a Rigaku D/Max-2500/PC diffractometer using Cu Kα as the radiation source with an operating voltage of 40 kV and current of 200 mA. Ultraviolet (UV) Raman spectra excited at 266 nm were acquired on a home-assembled UV Raman spectrograph with spectral resolution of 2 cm^{-1}. The power of the 266 nm laser on samples was close to 3.0 mW. Transmission electron microscopy (TEM) and high resolution transmission electron microscopy (HRTEM) images were obtained on a Tecnai G2 F30 S-Twin microscope (FEI Company) with an acceleration voltage of 300 kV. The Brunauer−Emmett−Teller (BET) specific surface areas were calculated based on the N_2 adsorption isotherms at 77 K performed on a Micromeritics ASAP 2000 apparatus. Ultraviolet and visible (UV−vis) diffuse reflectance spectra were obtained using a Cary 5000 spectrometer. Steady-state photoluminescence (PL) spectra were acquired on a FLS920 fluorescence spectrometer (Edinburgh Instruments) with the excitation line at 260 nm from a 450 W Xe lamp. Fourier transform infrared (FT-IR) spectra were recorded on a Thermo-Nicolet Nexus 470 FT-IR spectrometer. For the time-resolved (TR) mid-IR spectroscopic characterization, the Ga_2O_3 powder samples were uniformly dispersed on a CaF_2 plate at a density of 2 mg·cm^{-2}. A 266 nm laser with pulse duration of 6−8 ns (1 Hz, 1 mJ per pulse) was used to excite the samples. The TR-IR absorption spectra were recorded at room temperature on a Nicolet 870 FT-IR spectrometer equipped with a MCT (HgCdTe) detector by accumulating 60 traces repeated at 1 Hz. The decay curves were measured at a delay time from 50 ns to 100 μs.

Computational Methods. The density functional theory (DFT) calculations were performed by using the Vienna *ab initio* simulation package (VASP)[32,33] with the Perdew−Burke−Ernzerh parametrization of the generalized gradient approximation (GGA) adopted for the exchange correlation potential.[34] An energy cutoff of 520 eV was consistently used in our calculations. The atomic positions were fully relaxed with the conjugate gradient procedure until the residual forces vanished within 0.02 eV/Å. Pure γ-Ga_2O_3 and β-Ga_2O_3 were modeled with 3 × 3 × 1 and 3 × 9 × 5 grids for *k*-point sampling, respectively, while the γ/β phase-mixed heterostructure was modeled with a 2 × 2 × 1 grid for *k*-point sampling.

Photocatalytic Reaction. Photocatalytic overall water splitting reaction was performed in a closed gas circulation system. The photocatalyst powder (50 mg) was dispersed in

DOI: 10.1021/acs.jpcc.5b04092
J. Phys. Chem. C 2015, 119, 18221−18228

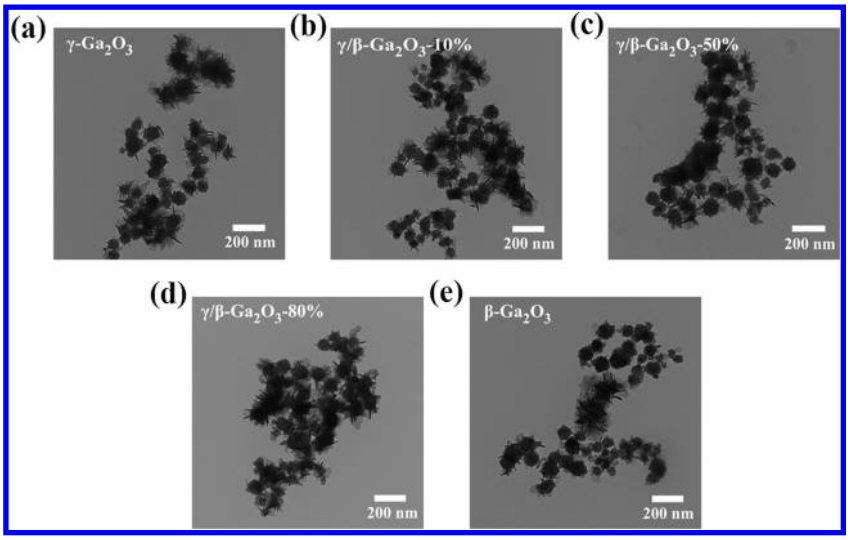

Figure 2. TEM images of γ-Ga_2O_3, phase-mixed γ/β-Ga_2O_3, and β-Ga_2O_3 samples.

well outgassed water (500 mL) by a magnetic stirrer in an inner irradiation vessel made of quartz. A 450 W high-pressure mercury lamp (USHIO UM452) was used as the irradiation light source. The reaction temperature was maintained at 287 ± 1 K by a continuous flow of cooling water. The amount of evolved H_2 and O_2 were determined by an online gas chromatograph (Shimadazu GC-8A, MS-5A column, TCD, Ar carrier).

RESULTS AND DISCUSSION

Figure 1a shows the powder XRD patterns of as-synthesized and calcined γ-Ga_2O_3 samples. The as-synthesized sample shows characteristic diffraction peaks at 2θ of 30.8°, 36.2°, 44.1°, 54.6°, 58.4°, and 64.2°, corresponding well with the standard PDF card of cubic γ-Ga_2O_3 (JCPDS card no. 20-0426). With γ-Ga_2O_3 calcined at 823 K for 0.75 h, these diffraction peaks show a 30% decrease in intensity; however, no obvious diffraction peaks from β-Ga_2O_3 are detected. This suggests the formation of a poorly crystalline, nanocrystalline, or amorphous phase that is not detected by powder XRD. This may be closely related to the inherently defective structure of γ phase in which different possible combinations of site occupations, giving different ratios of tetrahedral/octahedral gallium, may be present at the surface compared to the bulk.[31] As the calcination time is prolonged to 5 h, a diffraction peak at 31.7° attributed to monoclinic β-Ga_2O_3 (JCPDS card no. 41-1103) is clearly observed, indicating that a considerable amount of β-Ga_2O_3 is formed after calcination for 5 h. With the further increase of calcination time, the diffraction peaks from β-Ga_2O_3 become stronger, accompanied by a weakening of those from γ-Ga_2O_3. No diffraction peak attributed to γ-Ga_2O_3 is detected in the sample calcined for 24 h, suggesting that the transformation from γ to β phase is accomplished at this point.

UV Raman spectroscopy with an excitation line at 266 nm was also used to monitor the γ to β phase transformation of Ga_2O_3. Figure 1b shows the UV Raman spectra of as-synthesized and calcined γ-Ga_2O_3 samples. There are three broad bands at 340, 740, and 1610 cm^{-1} in the Raman spectrum of as-synthesized γ-Ga_2O_3. The bands at 340 and 740 cm^{-1} can be assigned to the bending and stretching of the Ga−O bond, while the band at 1610 cm^{-1} may be ascribed to the second-order Raman scattering. As for the sample calcined for 0.75 h, the Raman band at 198 cm^{-1} attributed to β-Ga_2O_3 is clearly observed, indicating the formation of β-Ga_2O_3.[20,35] The result is not in accordance with that revealed by the powder XRD, which must be due to the short-range structure sensitivity of Raman spectroscopy. With the calcination further proceeding, the Raman bands assigned to β-Ga_2O_3 and γ-Ga_2O_3 become stronger and weaker, respectively. The broad band at 1610 cm^{-1} attributed to γ-Ga_2O_3 is barely detected in the sample calcined for 11 h, and only Raman bands attributed to β-Ga_2O_3 is observed in the sample calcined for 24 h, indicating the accomplishment of phase transformation after calcination for 24 h.

Based on the XRD patterns and UV Raman spectra, the γ-Ga_2O_3 completely transforms into β-Ga_2O_3 after calcination for 24 h at 823 K; while the samples calcined for 0.75, 5, and 11 h are γ/β phase-mixed Ga_2O_3 with the estimated β phase contents of 10%, 50%, and 80%, respectively. In the following sections, the four samples will be labeled as γ/β-Ga_2O_3-10% (calcined for 0.75 h), γ/β-Ga_2O_3-50% (calcined for 5 h), γ/β-Ga_2O_3-80% (calcined for 11 h), and β-Ga_2O_3 (calcined for 24 h), respectively.

Besides the above characterizations, TEM images in Figure 2 show that the as-synthesized γ-Ga_2O_3 shows clusters of lamellates with overall spherical morphologies with an average size of 100 nm (Figure 2a), consistent with other reported samples prepared by the same method.[31] The morphology and size of Ga_2O_3 particles are maintained during the phase transformation (Figure 2b−e). Meanwhile, BET data (Table S1) show that the specific surface area decreases from 62.4 to 37.3 m^2/g when the γ-Ga_2O_3 is completely transformed into β-Ga_2O_3. Taken together, these results show that no significant agglomeration occurs in the phase transformation.

With the $Rh_{0.5}Cr_{1.5}O_3$ cocatalyst loaded, photocatalytic overall water splitting reaction was performed on these Ga_2O_3 photocatalysts. Figure 3 and Table 1 show the photocatalytic overall water splitting activities of Ga_2O_3 photocatalysts. All the photocatalysts can split water into H_2 and O_2 in an approximately stoichiometric ratio of 2:1. However, the photocatalytic activities are different. The γ-Ga_2O_3 photocatalyst shows a considerable photocatalytic activity with the H_2 evolution rate of 208.9 μmol/h and O_2 evolution rate of 93.6 μmol/h, and the surface-area normalized

DOI: 10.1021/acs.jpcc.5b04092
J. Phys. Chem. C 2015, 119, 18221−18228

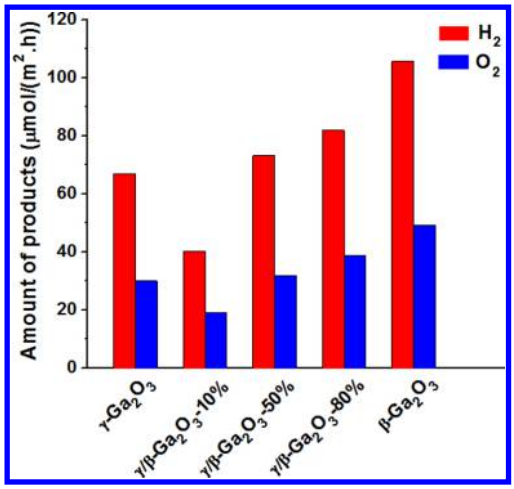

Figure 3. Photocatalytic overall water splitting activities of Ga_2O_3 photocatalysts with $Rh_{0.5}Cr_{1.5}O_3$ as the cocatalyst.

Table 1. H_2 and O_2 Evolution Rate of Ga_2O_3 Photocatalysts with $Rh_{0.5}Cr_{1.5}O_3$ as the Cocatalyst

samples	H_2 evolution rate (μmol/h)	O_2 evolution rate (μmol/h)	normalized H_2 evolution rate (μmol/(m^2·h))	normalized O_2 evolution rate (μmol/(m^2·h))
γ-Ga_2O_3	208.9	93.6	67.0	30.0
γ/β-Ga_2O_3-10%	127.4	60.5	40.4	19.2
γ/β-Ga_2O_3-50%	149.3	65.3	73.2	32.0
γ/β-Ga_2O_3-80%	154.0	72.9	81.9	38.8
β-Ga_2O_3	197.0	91.9	105.6	49.3
α-Ga_2O_3[a]			38	19
β-Ga_2O_3[a]			20	10
α/β-Ga_2O_3[a]			130	65

[a]Data from ref 17 (the cocatalyst was NiO_x prepared by an impregnation method). α/β-Ga_2O_3 represents Ga_2O_3 sample with the surface α/β phase junction. The activity of β-Ga_2O_3 photocatalyst with $Rh_{0.5}Cr_{1.5}O_3$ as the cocatalyst in this study is much higher than that of β-Ga_2O_3 photocatalyst with NiO_x as the cocatalyst in our previous study, which can be ascribed to the matched degree between Ga_2O_3 material and cocatalyst, and $Rh_{0.5}Cr_{1.5}O_3$ cocatalyst is much better than NiO_x cocatalyst for β-Ga_2O_3 photocatalyst.[30]

evolution rate for H_2 and O_2 are 67.0 and 30.0 μmol/(m^2·h), respectively. With a small amount of γ phase transformed into β phase, the photocatalytic activity decreases by 40% for the γ/β-Ga_2O_3-10% photocatalyst, which is the lowest photocatalytic overall water splitting activity among the tested photocatalysts, no matter whether the activity is normalized by specific surface area or not. As the amount of β phase further increases, the activity increases gradually. However, a remarkable enhancement of photocatalytic activity is observed once γ phase is completely transformed into β phase, and the β-Ga_2O_3 photocatalyst shows the highest normalized activity with the H_2 evolution rate of 105.6 μmol/(m^2·h) and O_2 evolution rate of 49.3 μmol/(m^2·h).

The water splitting reaction was also carried out on these Ga_2O_3 photocatalysts with photodeposited Ni as the cocatalyst. In contrast to the situation with $Rh_{0.5}Cr_{1.5}O_3$ as the cocatalyst, the γ-Ga_2O_3 photocatalyst shows a higher normalized activity than the β-Ga_2O_3 photocatalyst, which can be ascribed to the matched degree between Ga_2O_3 material and cocatalyst.[30] However, the γ/β-Ga_2O_3-10% photocatalyst still shows the lowest photocatalytic overall water splitting activity (Figure S1). Therefore, the lowest activity for the γ/β-Ga_2O_3-10% photocatalyst and the variation tendency of photocatalytic activity cannot be just ascribed to the difference in relative amount of γ and β phases but must be associated with the intrinsic phase property of Ga_2O_3 photocatalyst.

The situation for the γ/β-Ga_2O_3 system is vastly different from that for the reported α/β-Ga_2O_3 system. As shown in Table 1, the photocatalytic activity of α/β-Ga_2O_3 photocatalyst in the early stages of phase transformation reaches up to several times of α-Ga_2O_3 or β-Ga_2O_3 due to the surface α/β phase junction. To better understand the effect of phase junction, we performed further studies to understand why the γ/β-Ga_2O_3-10% photocatalyst shows the lowest activity.

Figure 4 shows the UV−vis diffuse reflectance spectra of Ga_2O_3 samples. Although all the samples show a similar

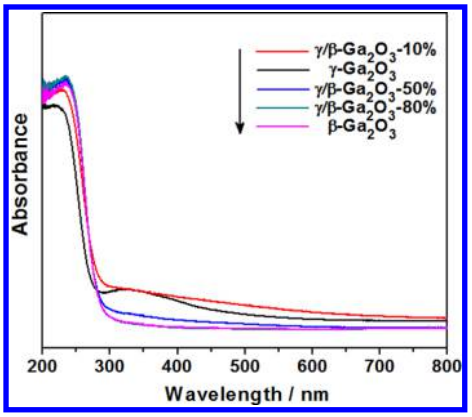

Figure 4. UV−vis diffuse reflectance spectra of γ-Ga_2O_3, phase-mixed γ/β-Ga_2O_3, and β-Ga_2O_3 samples.

absorption below 300 nm, there are a few differences in the range above 300 nm. The γ-Ga_2O_3 sample has a weak absorption band at 350 nm. Due to the intrinsic bandgap of about 4.6 eV for γ-Ga_2O_3, the weak band can be attributed to the absorption of defect states. With a small amount of γ-Ga_2O_3 transformed into β-Ga_2O_3, the weak band converts into a noteworthy tailing absorption in the 300−600 nm region. As the amount of β phase is gradually increased, the tailing absorption becomes progressively weaker, and no difference is observed between the γ/β-Ga_2O_3-80% and β-Ga_2O_3 samples. Therefore, apart from the difference in phase composition, the variation in tailing absorption reflects some differences in the states of these Ga_2O_3 samples.

Figure 5 shows the PL spectra of these Ga_2O_3 samples excited at 260 nm. The γ-Ga_2O_3 sample has a broad emission band at 470 nm. For the γ/β-Ga_2O_3-10% sample, the PL band shifts to 535 nm. With the content of β phase increasing, the broad emission band at 505 nm is observed for the γ/β-Ga_2O_3-50%, γ/β-Ga_2O_3-80%, and β-Ga_2O_3 samples, and the band becomes stronger. According to the literature,[20,36,37] the emission band of γ-Ga_2O_3 sample can be attributed to the recombination of an electron on a donor formed by an oxygen vacancy and a hole on an acceptor formed by either a gallium vacancy or gallium−oxygen vacancy pairs. To assign the PL bands of calcined Ga_2O_3 samples, additional experiments were performed. No band attributed to 2-aminoethanol (the solvent) is observed in the IR spectrum of as-synthesized γ-Ga_2O_3 by solvothermal method (Figure S2). Meanwhile, the γ-Ga_2O_3 and γ/β-Ga_2O_3-10% samples calcined at 723 K for 4 h under an atmosphere of oxygen show almost the same emission band as

DOI: 10.1021/acs.jpcc.5b04092
J. Phys. Chem. C 2015, 119, 18221−18228

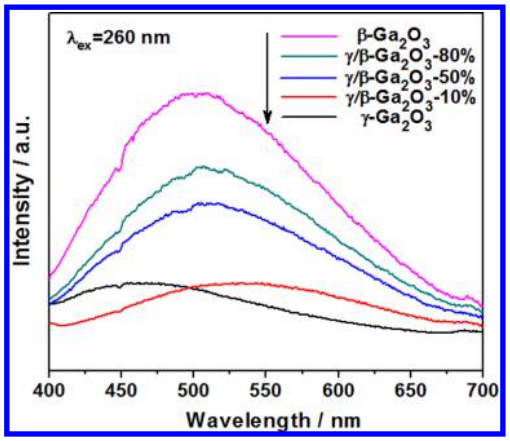

Figure 5. Photoluminescence spectra of γ-Ga_2O_3, phase-mixed γ/β-Ga_2O_3, and β-Ga_2O_3 samples.

the γ/β-Ga_2O_3-10% sample (Figure S3). These results indicate that the emission band for calcined γ-Ga_2O_3 samples can be assigned to defect states formed during the phase transformation. The differences in PL band and intensity mean that there are indeed some differences in defect states between these Ga_2O_3 samples.

Figure 6 shows the HRTEM images of Ga_2O_3 samples. The (220) planes with interplanar distance of 2.90 Å are present in the HRTEM image of γ-Ga_2O_3 sample (Figure 6a). The β-Ga_2O_3 sample shows characteristic (002) planes with interplanar distance of 2.82 Å in its HRTEM image (Figure 6e). For the phase-mixed samples, the (002) and (111) planes attributed to β phase are clearly observed in the HRTEM images of the γ/β-Ga_2O_3-10% and γ/β-Ga_2O_3-50% samples (Figure 6b,c), respectively, while no plane attributed to γ phase is detected for the γ/β-Ga_2O_3-80% sample (Figure 6d), which means that the surface region of γ/β-Ga_2O_3-80% sample may be only composed of β phase.

In comparison with γ-Ga_2O_3 sample, there is significant disordered structure observed between γ and β phases for the γ/β-Ga_2O_3-10% sample. With the amount of β phase increasing, the disordered structure becomes less and finally disappears in the β-Ga_2O_3 sample. In contrast, in our previous study of phase transformation of α-Ga_2O_3 to β-Ga_2O_3, there was no obviously disordered structure observed in the α/β phase-mixed Ga_2O_3 samples.[17,35] Since the lattice mismatch between γ-Ga_2O_3 and β-Ga_2O_3 (2.75%) is almost as small as that between α-Ga_2O_3 and β-Ga_2O_3 (2.05%), the appearance of disordered structure during the phase transformation of γ-Ga_2O_3 to β-Ga_2O_3 cannot be ascribed to the lattice mismatch but may be related to the inherently defective spinel structure of γ-Ga_2O_3.[31] This viewpoint is also supported by the fact that disordered structure was observed in the phase transformation of γ-Al_2O_3 with the structure the same as γ-Ga_2O_3.[38,39] Based on the above data, it is proposed that the differences in UV−vis and PL spectra between Ga_2O_3 samples may reflect the disordered structure, which might greatly influence the dynamic behavior of photogenerated carriers, thus leading to the difference in photocatalytic overall water splitting activity.

To better understand the structure−activity relationship, we performed DFT calculations to explore the geometrical and electronic properties of γ-Ga_2O_3, phase-mixed γ/β-Ga_2O_3 and β-Ga_2O_3. The structures of pure γ-Ga_2O_3 and β-Ga_2O_3 were first optimized using the published crystal structures as starting points: for γ-Ga_2O_3 the defective spinel structure with $Fd\bar{3}m$ symmetry,[31] and the monoclinic structure with $C2/m$ symmetry for β-Ga_2O_3.[26] Figure S4 displays the density of states (DOS) of pure β-Ga_2O_3 and the three most stable configurations of γ-Ga_2O_3 similar to theoretical structure of γ-Al_2O_3 reported in the literature.[40] The γ-Ga_2O_3 with any of the three configurations shows a smaller bandgap than that of β-Ga_2O_3 because the defect states associated with the vacancies exist in its gap. To investigate the phase-mixed γ/β-Ga_2O_3, we constructed the computational model similar to our previous study on α/β phase junction of Ga_2O_3.[41] Due to the defective structure characteristic of γ-Ga_2O_3, there are two types of vacancy sites (**1** and **2**) for the most stable model (Figure 7a). This indicates that the structure may suffer great changes even below the phase transformation temperature, and the appearance of disordered structure between γ and β phases during the phase transformation may be closely related to the structure. Figure 7b,c shows the DOSs of the models with different axis angles. It can be seen that the bandgap of γ/β phase-mixed Ga_2O_3 is much smaller than that of pure γ-Ga_2O_3

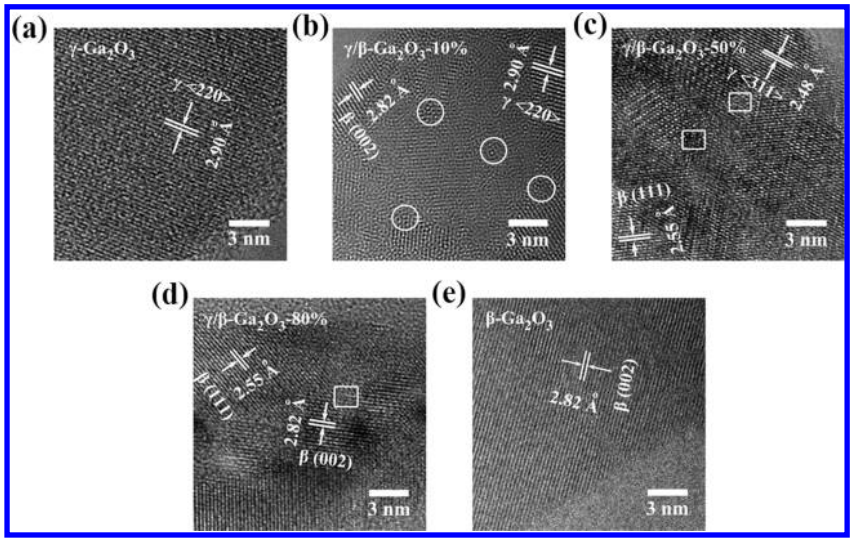

Figure 6. HRTEM images of γ-Ga_2O_3, phase-mixed γ/β-Ga_2O_3, and β-Ga_2O_3 samples (the areas scaled out by circular and square symbols are the disordered structure).

DOI: 10.1021/acs.jpcc.5b04092
J. Phys. Chem. C 2015, 119, 18221−18228

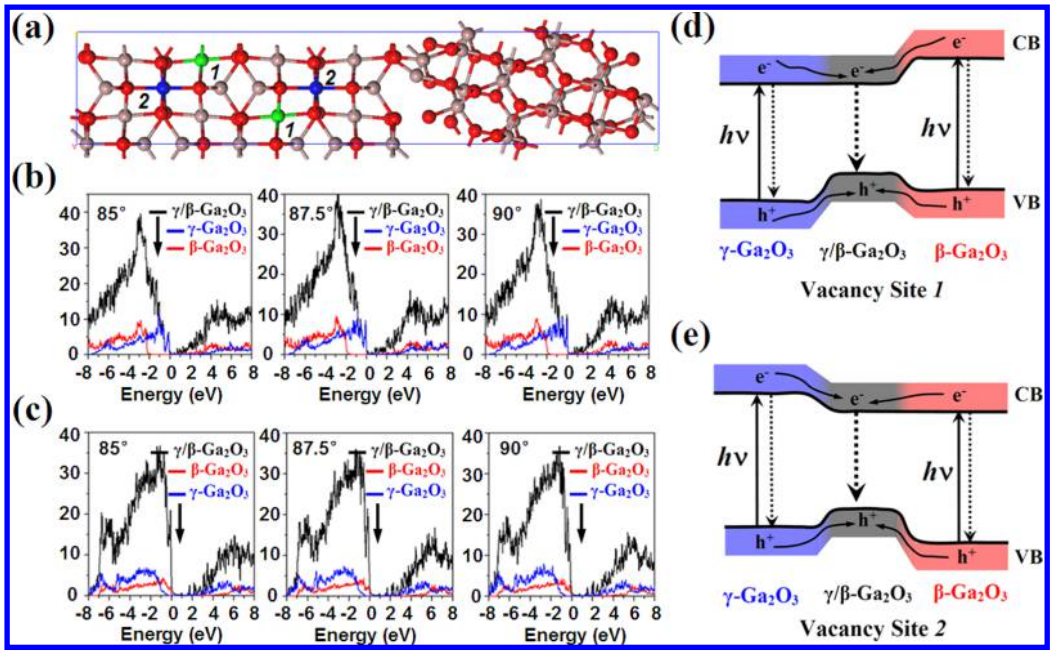

Figure 7. (a) Constructed model for the calculation of phase-mixed γ/β-Ga_2O_3 (the green and blue sites represent the vacancy sites **1** and **2**, respectively). (b) DOSs of a most stable phase-mixed model (vacancy site **1**) with different axis angles. (c) DOSs of a most stable phase-mixed model (vacancy site **2**) with different axis angles (d) Schematic representation of band alignment for the situation of vacancy site **1**. (e) Schematic representation of band alignment for the situation of vacancy site **2**.

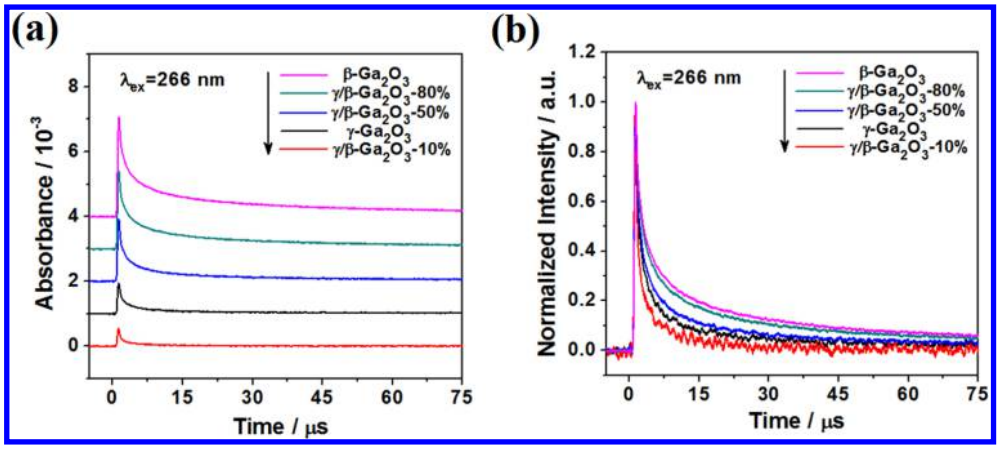

Figure 8. Non-normalized (a) and normalized (b) TR mid-IR absorption decay curves of Ga_2O_3 samples.

and β-Ga_2O_3. Interestingly, the band alignment of γ-Ga_2O_3 and β-Ga_2O_3 is almost opposite for the situation of **1** and **2** vacancy sites, which means that there may be a large fluctuation of electronic potential in the γ/β phase-mixed region. As Figure 7d,e show, the junctions between the Ga_2O_3 with disordered structure and β-Ga_2O_3 (γ-Ga_2O_3) show type-I band alignments, which are unfavorable for charge transfer, instead, result in severe charge recombination. Such a situation was not found for the α/β-Ga_2O_3 system.[41] Owing to the well matched structures, the α/β phase junction shows a type-II band alignment and facilitates charge separation. This may be the reason for the photocatalytic activity decreased in the γ/β-Ga_2O_3 system and increased in the α/β-Ga_2O_3 system.

Time-resolved (TR) mid-IR absorption spectroscopy is a powerful technique for studying the kinetics of photogenerated electrons in photocatalysts.[42,43] As for microsecond-scaled TR mid-IR spectroscopy, the initial IR absorbance can directly reflect the amount of long-lived electrons on shallow traps or defects, etc. Figure 8a,b shows the non-normalized and normalized TR mid-IR absorption decay curves of Ga_2O_3 samples, respectively. In general, with the amount of β phase increasing, the initial IR absorbance becomes greater and the decay of photogenerated electrons becomes slower. However, the γ/β-Ga_2O_3-10% sample shows the lowest initial IR absorbance and the fastest decay of photogenerated electrons among these Ga_2O_3 samples, which means the least long-lived photogenerated electrons survived from recombination until 50 ns. As for Ga_2O_3 based photocatalysts, the long-lived photogenerated electron is assumed to be favorable for photocatalytic reactions.[17,29] Since the γ/β-Ga_2O_3-10% sample with the maximum disordered structure shows the lowest initial IR absorbance and activity, it can be inferred that the disordered structure serves as the recombination centers causing the decrease of activity. Once all the disordered structure is eliminated, the photocatalytic activity of β-Ga_2O_3 sample is enhanced obviously.

DOI: 10.1021/acs.jpcc.5b04092
J. Phys. Chem. C 2015, 119, 18221−18228

From the above characterizations and theoretical calculations, we can conclude that the lowest activity of γ/β-Ga_2O_3-10% photocatalyst is attributed to the severe charge recombination caused by the disordered structure between γ and β phases, and the appearance of disordered structure during the phase transformation of γ-Ga_2O_3 to β-Ga_2O_3 is closely associated with the defective spinel structure of γ-Ga_2O_3. Based on the analysis of α/β-Ga_2O_3 and γ/β-Ga_2O_3 systems, we propose that two requirements should be met for the construction of phase junction being beneficial for photocatalytic reactions: (1) The interfacial structure between two phases should not be disordered or defective, but be well matched; (2) The junction should have a type-II band alignment for efficient charge separation. It is anticipated that more efficient photoconversion systems based on phase junction structures can be developed as long as these requirements are satisfied.

CONCLUSIONS

In summary, with Ga_2O_3 photocatalyst as an example, we have investigated the effect of phase junction structure on photocatalytic performance in overall water splitting. All the Ga_2O_3 photocatalysts with pure γ and β phases and mixed γ/β phase can split water into H_2 and O_2 stoichiometrically; however, the γ/β-Ga_2O_3 photocatalyst with low content of β phase shows the lowest activity. The spectroscopic and HRTEM characterizations indicate that there is significant disordered structure between the γ and β phases in the γ/β-Ga_2O_3 photocatalyst with a small amount of β phase present. TR-IR spectroscopic characterization and theoretical calculations indicate that the disordered structure serves as charge recombination sites decreasing the photocatalytic activity. Through the analysis of γ/β-Ga_2O_3 and reported α/β-Ga_2O_3 systems, we propose two necessities for the construction of phase junction being beneficial for photocatalytic reactions: nondefective, well-matched interfacial structure, and type-II band alignment between two phases.

ASSOCIATED CONTENT

Supporting Information

The Supporting Information is available free of charge on the ACS Publications website at DOI: 10.1021/acs.jpcc.5b04092.

BET data, photocatalytic activity (Ni as the cocatalyst), IR spectra, PL spectra, and the DOSs of Ga_2O_3 samples (PDF)

AUTHOR INFORMATION

Corresponding Author

*E-mail: canli@dicp.ac.cn. Fax: +86-411-84694447. Tel: +86-411-84379070. Homepage: www.canli.dicp.ac.cn.

Notes

The authors declare no competing financial interest.

ACKNOWLEDGMENTS

This work was financially supported by the National Basic Research Program of China (No. 2014CB239403) and the National Natural Science Foundation of China (No. 21090340, 21373209, and 21203185).

REFERENCES

(1) Kudo, A.; Miseki, Y. Heterogeneous Photocatalyst Materials for Water Splitting. *Chem. Soc. Rev.* **2009**, *38*, 253−278.

(2) Maeda, K.; Domen, K. Photocatalytic Water Splitting: Recent Progress and Future Challenges. *J. Phys. Chem. Lett.* **2010**, *1*, 2655−2661.

(3) Chen, X. B.; Shen, S. H.; Guo, L. J.; Mao, S. S. Semiconductor-based Photocatalytic Hydrogen Generation. *Chem. Rev.* **2010**, *110*, 6503−6570.

(4) Li, X.; Yu, J. G.; Low, J. X.; Fang, Y. P.; Xiao, J.; Chen, X. B. Engineering Heterogeneous Semiconductors for Solar Water Splitting. *J. Mater. Chem. A* **2015**, *3*, 2485−2534.

(5) Kato, H.; Asakura, K.; Kudo, A. Highly Efficient Water Splitting into H_2 and O_2 over Lanthanum-doped $NaTaO_3$ Photocatalysts with High Crystallinity and Surface Nanostructure. *J. Am. Chem. Soc.* **2003**, *125*, 3082−3089.

(6) Takata, T.; Domen, K. Defect Engineering of Photocatalysts by Doping of Aliovalent Metal Cations for Efficient Water Splitting. *J. Phys. Chem. C* **2009**, *113*, 19386−19388.

(7) Ye, H. C.; Park, H. S.; Bard, A. J. Screening of Electrocatalysts for Photoelectrochemical Water Oxidation on W-doped $BiVO_4$ Photocatalysts by Scanning Electrochemical Microscopy. *J. Phys. Chem. C* **2011**, *115*, 12464−12470.

(8) Chen, X. B.; Liu, L.; Yu, P. Y.; Mao, S. S. Increasing Solar Absorption for Photocatalysis with Black Hydrogenated Titanium Dioxide Nanocrystals. *Science* **2011**, *331*, 746−750.

(9) Yang, J. H.; Wang, D. E.; Han, H. X.; Li, C. Roles of Cocatalysts in Photocatalysis and Photoelectrocatalysis. *Acc. Chem. Res.* **2013**, *46*, 1900−1909.

(10) Li, R. G.; Zhang, F. X.; Wang, D. E.; Yang, J. X.; Li, M. R.; Zhu, J.; Zhou, X.; Han, H. X.; Li, C. Spatial Separation of Photogenerated Electrons and Holes among {010} and {110} Crystal Facets of $BiVO_4$. *Nat. Commun.* **2013**, *4*, 1432.

(11) Hwang, D. W.; Lee, J. S.; Li, W.; Oh, S. H. Electronic Band Structure and Photocatalytic Activity of $Ln_2Ti_2O_7$ (Ln = La, Pr, Nd). *J. Phys. Chem. B* **2003**, *107*, 4963−4970.

(12) Sato, J.; Kobayashi, H.; Inoue, Y. Photocatalytic Activity for Water Decomposition of Indates with Octahedrally Coordinated d^{10} Configuration. II. Roles of Geometric and Electronic Structures. *J. Phys. Chem. B* **2003**, *107*, 7970−7975.

(13) Abe, R.; Higashi, M.; Zou, Z. G.; Sayama, K.; Abe, Y.; Arakawa, H. Photocatalytic Water Splitting into H_2 and O_2 over R_3TaO_7 and R_3NbO_7 (R = Y, Yb, Gd, La): Effect of Crystal Structure on Photocatalytic Activity. *J. Phys. Chem. B* **2004**, *108*, 811−814.

(14) Yoshioka, K.; Petrykin, V.; Kakihana, M.; Kato, H.; Kudo, A. The Relationship between Photocatalytic Activity and Crystal Structure in Strontium Tantalates. *J. Catal.* **2005**, *232*, 102−107.

(15) Hu, C. C.; Tsai, C. C.; Teng, H. S. Structure Characterization and Tuning of Perovskite-like $NaTaO_3$ for Applications in Photoluminescence and Photocatalysis. *J. Am. Ceram. Soc.* **2009**, *92*, 460−466.

(16) Zhang, J.; Xu, Q.; Feng, Z. C.; Li, M. J.; Li, C. Importance of the Relationship between Surface Phases and Photocatalytic Activity of TiO_2. *Angew. Chem., Int. Ed.* **2008**, *47*, 1766−1769.

(17) Wang, X.; Xu, Q.; Li, M. R.; Shen, S.; Wang, X. L.; Wang, Y. C.; Feng, Z. C.; Shi, J. Y.; Han, H. X.; Li, C. Photocatalytic Overall Water Splitting Promoted by an α-β Phase Junction on Ga_2O_3. *Angew. Chem., Int. Ed.* **2012**, *51*, 13089−13092.

(18) Takahara, I.; Saito, M.; Inaba, M.; Murata, K. Effects of Pretreatment of a Silica-supported Gallium Oxide Catalyst with H_2 on Its Catalytic Performance for Dehydrogenation of Propane. *Catal. Lett.* **2004**, *96*, 29−32.

(19) Zheng, B.; Hua, W. M.; Yue, Y. H.; Gao, Z. Dehydrogenation of Propane to Propene over Different Polymorphs of Gallium Oxide. *J. Catal.* **2005**, *232*, 143−151.

(20) Hou, Y. D.; Wu, L.; Wang, X. C.; Ding, Z. X.; Li, Z. H.; Fu, X. Z. Photocatalytic Performance of α-, β-, and γ-Ga_2O_3 for the Destruction of Volatile Aromatic Pollutants in Air. *J. Catal.* **2007**, *250*, 12−18.

(21) Yanagida, T.; Sakata, Y.; Imamura, H. Photocatalytic Decomposition of H_2O into H_2 and O_2 over Ga_2O_3 Loaded with NiO. *Chem. Lett.* **2004**, *33*, 726−727.

DOI: 10.1021/acs.jpcc.5b04092
J. Phys. Chem. C 2015, 119, 18221−18228

(22) Sakata, Y.; Matsuda, Y.; Yanagida, T.; Hirata, K.; Imamura, H.; Teramura, K. Effect of Metal Ion Addition in a Ni Supported Ga_2O_3 Photocatalyst on the Photocatalytic Overall Splitting of H_2O. *Catal. Lett.* **2008**, *125*, 22−26.
(23) Filippo, E.; Tepore, M.; Baldassarre, F.; Siciliano, T.; Micocci, G.; Quarta, G.; Calcagnile, L.; Tepore, A. Synthesis of β-Ga_2O_3 Microstructures with Efficient Photocatalytic Activity by Annealing of GaSe Single Crystal. *Appl. Surf. Sci.* **2015**, *338*, 69−74.
(24) Liu, J.; Zhang, G. K. Mesoporous Mixed-phase Ga_2O_3: Green Synthesis and Enhanced Photocatalytic Activity. *Mater. Res. Bull.* **2015**, *68*, 254−259.
(25) Roy, R.; Hill, V. G.; Osborn, E. F. Polymorphism of Ga_2O_3 and the System Ga_2O_3-H_2O. *J. Am. Chem. Soc.* **1952**, *74*, 719−722.
(26) Playford, H. Y.; Hannon, A. C.; Barney, E. R.; Walton, R. I. Structures of Uncharacterised Polymorphs of Gallium Oxide from Total Neutron Diffraction. *Chem. - Eur. J.* **2013**, *19*, 2803−2813.
(27) Hisatomi, T.; Miyazaki, K.; Takanabe, K.; Maeda, K.; Kubota, J.; Sakata, Y.; Domen, K. Isotopic and Kinetic Assessment of Photocatalytic Water Splitting on Zn-added Ga_2O_3 Photocatalyst Loaded with $Rh_{2-y}Cr_yO_3$ Cocatalyst. *Chem. Phys. Lett.* **2010**, *486*, 144−146.
(28) Sakata, Y.; Matsuda, Y.; Nakagawa, T.; Yasunaga, R.; Imamura, H.; Teramura, K. Remarkable Improvement of the Photocatalytic Activity of Ga_2O_3 Towards the Overall Splitting of H_2O. *ChemSusChem* **2011**, *4*, 181−184.
(29) Wang, X.; Shen, S.; Jin, S. Q.; Yang, J. X.; Li, M. R.; Han, H. X.; Li, C. Effects of Zn^{2+} and Pb^{2+} Dopants on the Activity of Ga_2O_3-based Photocatalysts for Water Splitting. *Phys. Chem. Chem. Phys.* **2013**, *15*, 19380−19386.
(30) Sakata, Y.; Nakagawa, T.; Nagamatsu, Y.; Matsuda, Y.; Yasunaga, R.; Nakao, E.; Imamura, H. Photocatalytic Properties of Gallium Oxides Prepared by Precipitation Methods toward the Overall Splitting of H_2O. *J. Catal.* **2014**, *310*, 45−50.
(31) Playford, H. Y.; Hannon, A. C.; Tucker, M. G.; Dawson, D. M.; Ashbrook, S. E.; Kastiban, R. J.; Sloan, J.; Walton, R. I. Characterization of Structural Disorder in γ-Ga_2O_3. *J. Phys. Chem. C* **2014**, *118*, 16188−16198.
(32) Kresse, G.; Hafner, J. *Ab. Initio* Molecular Dynamics for Liquid Metals. *Phys. Rev. B: Condens. Matter Mater. Phys.* **1993**, *47*, 558−561.
(33) Blöchl, P. E. Projector Augmented-wave Method. *Phys. Rev. B: Condens. Matter Mater. Phys.* **1994**, *50*, 17953−17979.
(34) Perdew, J. P.; Burke, K.; Ernzerhof, M. Generalized Gradient Approximation Made Simple. *Phys. Rev. Lett.* **1996**, *77*, 3865−3868.
(35) Wang, X.; Xu, Q.; Fan, F. T.; Li, M. R.; Feng, Z. C.; Li, C. Study of the Phase Transformation of Single Particles of Ga_2O_3 by UV-Raman Spectroscopy and High-Resolution TEM. *Chem. - Asian J.* **2013**, *8*, 2189−2195.
(36) Harwig, T.; Kellendonk, F. Some Observations on the Photoluminescence of Doped β-Galliumsesquioxide. *J. Solid State Chem.* **1978**, *24*, 255−263.
(37) Binet, L.; Gourier, D. Origin of the Blue Luminescence of β-Ga_2O_3. *J. Phys. Chem. Solids* **1998**, *59*, 1241−1249.
(38) Damani, R. J.; Makroczy, P. Heat Treatment Induced Phase and Microstructural Development in Bulk Plasma Sprayed Alumina. *J. Eur. Ceram. Soc.* **2000**, *20*, 867−888.
(39) Düvel, A.; Romanova, E.; Sharifi, M.; Freude, D.; Wark, M.; Heitjans, P.; Wilkening, M. Mechanically Induced Phase Transformation of γ-Al_2O_3 into α-Al_2O_3. Access to Structurally Disordered γ-Al_2O_3 with a Controllable Amount of Pentacoordinated Al Sites. *J. Phys. Chem. C* **2011**, *115*, 22770−22780.
(40) Gutierrez, G.; Taga, A.; Johansson, B. Theoretical Structure Determination of γ-Al_2O_3. *Phys. Rev. B: Condens. Matter Mater. Phys.* **2001**, *65*, 012101.
(41) Ju, M. G.; Wang, X.; Liang, W. Z.; Zhao, Y.; Li, C. Tuning the Energy Band-gap of Crystalline Gallium Oxide to Enhance Photocatalytic Water Splitting: Mixed-phase Junctions. *J. Mater. Chem. A* **2014**, *2*, 17005−17014.
(42) Yamakata, A.; Ishibashi, T.; Onishi, H. Electron- and Hole-capture Reactions on Pt/TiO_2 Photocatalyst Exposed to Methanol Vapor Studied with Time-resolved Infrared Absorption Spectroscopy. *J. Phys. Chem. B* **2002**, *106*, 9122−9125.
(43) Chen, T.; Feng, Z. C.; Wu, G. P.; Shi, J. Y.; Ma, G. J.; Ying, P. L.; Li, C. Mechanistic Studies of Photocatalytic Reaction of Methanol for Hydrogen Production on Pt/TiO_2 by in situ Fourier Transform IR and Time-resolved IR Spectroscopy. *J. Phys. Chem. C* **2007**, *111*, 8005−8014.

DOI: 10.1021/acs.jpcc.5b04092
J. Phys. Chem. C 2015, 119, 18221−18228